TRANSIENT, FOCAL ACCUMULATION OF AXONAL MITOCHONDRIA DURING THE EARLY STAGES OF WALLERIAN DEGENERATION

HENRY DEF. WEBSTER, M.D.

From the Department of Neurology, Harvard Medical School and the Neurology Service and the Edwin S. Webster Memorial Laboratory of the Department of Pathology, Massachusetts General Hospital, Boston

ABSTRACT

Wallerian degeneration was produced in guinea pig sciatic nerves by a crush injury. At intervals of 2, 12, 24, 36, 48, 72, and 96 hours after the crush, the nerves were fixed in osmium tetroxide, and blocks from the distal, degenerating segment identified topographically prior to embedding in Araldite or Epon. Phase and electron microscopic study of serial cross- and longitudinal sections reveals a striking, localized accumulation of axonal mitochondria which precedes or accompanies the swelling and fragmentation previously reported by others. These focal accumulations of mitochondria are transient and are most frequently observed in the paranodal axoplasm of large myelinated fibers 24 to 36 hours after crush injury, but are also occasionally identified in small myelinated fibers and unmyelinated axons. Migration and proliferation of axonal mitochondria are considered as possible explanations of these observations.

INTRODUCTION

A topographical phase and electron microscopic study of Wallerian degeneration (the axonal disintegration and demyelination that occur distal to a site of peripheral nerve injury) was undertaken in order to gain further insight into the cellular mechanism of demyelination in peripheral nerve. During the course of this study, which was limited to the early stages of this process, a striking, localized accumulation of axonal mitochondria was observed that preceded or accompanied the mitochondrial swelling and fragmentation previously reported by others (28, 14).

Although the ultrastructure of mitochondria in normal peripheral nerve axons and their concentration at nodes of Ranvier and terminal endings are well known (13, 25, 2, 6), few observations are currently available on the sequential alterations in number, size, shape, and internal structure of axonal mitochondria during a pathological process. Mitochondrial swelling and fragmentation, which are commonly observed features of cellular pathology, have been described most frequently. In addition, electron micrographs showing an increase in the number of axonal mitochondria have been included in two studies of experimental allergic encephalomyelitis. This appearance was identified by Condie and Good as the earliest pathological change (7), while Luse and McDougal interpreted it as the growth cone of an axonal sprout and did not relate it specifically to this disease process (18).

MATERIALS AND METHODS

In our first experiments, light and phase microscopic study of serial longitudinal sections stained for axons (Bodian method) and myelin sheaths (2 per cent buffered osmium tetroxide) demonstrated that: 1, axons and myelin sheaths are normal in sham-operated control animals; 2, following surgical division of the sciatic nerve, retraction and hemorrhage resulted in severe distortion of individual nerve fibers in the degenerating, distal segment; 3, interruption of axons and myelin sheaths by a crush injury and the use of *in situ* fixation prevented this distortion and made possible study of individual fibers over long distances; 4, destruction of axons and myelin sheaths was complete in the crush zone; 5, the sequence of distal axon and myelin disintegration was similar to that seen after surgical division of guinea pig sciatic nerves. The choice of this crush method for producing Wallerian degeneration, the sampling technique, and the procedure for blocking the nerves for topographic phase and electron microscopic study were determined by these initial observations.

Adult male Hartley guinea pigs weighing 250 to 350 gm were utilized in order to facilitate comparison of results with those obtained in a study of experimental diphtheritic neuritis (30). They were caged in groups of four and fed Purina chow and water *ad lib*. With the animal under ether anesthesia, both sciatic nerves of each experimental guinea pig were surgically exposed at their origin and crushed over a 2-millimeter distance for 5 seconds with a fine hemostat. The sciatic nerves of control animals were exposed bilaterally in similar fashion. The incisions were closed with collodion and remained free of infection.

At intervals of 12, 24, 36, 48, 72, and 96 hours after the crush, the sciatic nerves of experimental animals were exposed, fixed in 2 per cent osmium tetroxide, dehydrated in acetone, and embedded in Araldite, according to the procedure previously reported (30). Subsequently, after appropriate study of normal and control material, additional sciatic nerves were crushed, exposed 2 hours later, and fixed in similar fashion prior to embedding in Epon (17). For the study of the axonal and myelin degeneration topographically, each nerve was divided into blocks according to Fig. 1. The proximal portion (*P*) of the nerve included the crush and 4 to 8 mm of nerve distal to it. The next portion, measuring 5 to 7 mm, was divided into six individually numbered

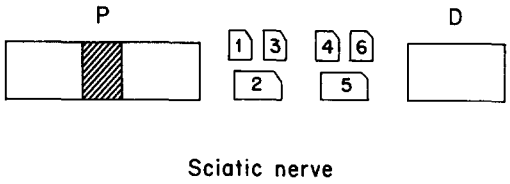

FIGURE 1

Diagram of guinea pig sciatic nerve showing the relationship of the crush (shaded area) to blocks utilized for topographic study by light (*P* and *D*), phase and electron (*1* to *6*) microscopy.

blocks and the distal end of each was identified by notching. Sections from these blocks were studied by phase and electron microscopy. Numbers *1*, *3*, *4*, and *6* were used for longitudinal sections, and cross-sections were cut from the proximal ends of blocks *2* and *5*. The distal portion (*D*) varied in length from 3 to 5 mm and, along with (*P*), was embedded in paraffin and sectioned longitudinally for study by light microscopy.

A few sciatic nerves from the sham-operated controls were studied as above but absence of lesions made it unnecessary to pursue this procedure. Blocks from the remaining control nerves were not topographically identified.

Sciatic nerves from additional experimental and

FIGURE 2

Longitudinal section, normal paranodal region, stained with lead hydroxide. The paranodal axoplasm contains a mitochondrion (*M*) bounded by a double membrane. Longitudinal orientation of some cristae is apparent. Filaments (*F*) and vesicular profiles are also present in axoplasm. The myelin lamellae terminate at the axon surface in loops formed by splitting of the major dense line. A small protrusion of axoplasm is surrounded by the outer four myelin lamellae which form a long, redundant loop within Schwann cell cytoplasm (*SC*). × 103,000.

FIGURE 3

Cross-section, normal myelinated fiber, stained with lead hydroxide. Two axonal mitochondria show variation in the spacing of limiting membranes, array of cristae, and matrix density. × 79,000.

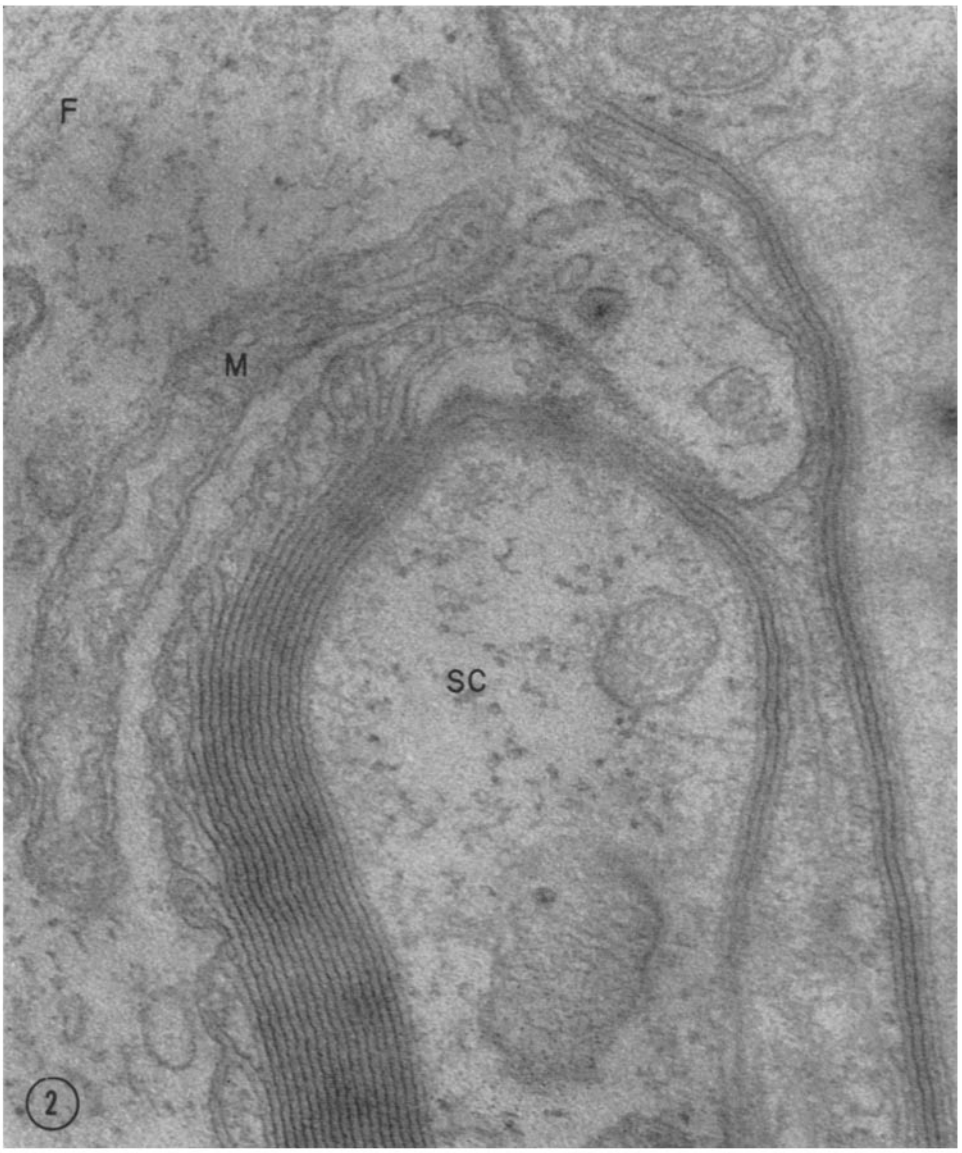
F
M
SC
2

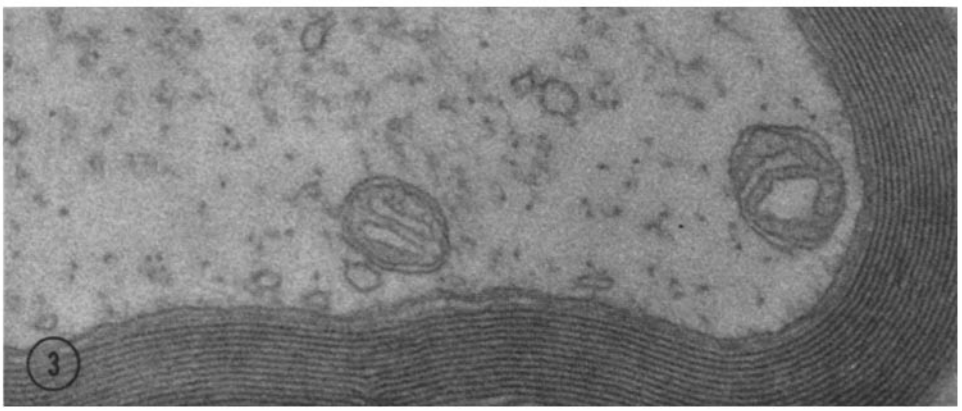
3

control animals were fixed in formalin and stained by conventional neuropathological techniques.

OBSERVATIONS

Thirty to 45 serial sections, 2 microns thick, from each of the six blocks were utilized in studying the sequential, topographic alterations in the distal axons and myelin sheaths at intervals of 2, 12, 24, 36, 48, 72, and 96 hours after a crush injury. Although sections from 6 to 15 nerves were available for each of these intervals, those from 3 to 5 nerves were selected for detailed study, subsequent thin sectioning, and electron microscopy. The results and correlation of these observations with earlier histopathologic and electron microscopic studies of Wallerian degeneration will be published elsewhere.

Normal Sciatic Nerve

The phase microscopic appearance of normal, osmium tetroxide–fixed, guinea pig sciatic nerve has been reviewed recently (29). In longitudinal section, axonal mitochondria may appear as randomly distributed threads oriented in the long axis of the nerve fiber.

The electron microscopic morphology of axonal mitochondria in our normal material is similar to that previously reported in neurons (23) and is shown in Figs. 2 and 3. Their size depends on the plane of section, their diameter varying from 0.15 to 0.3 microns and their length being several microns. They are bounded by a double membrane, the inner of which is folded to form cristae which frequently are oriented longitudinally. Mitochondria are frequently concentrated at nodes of Ranvier, confirming earlier observations of others (25). The morphology of mitochondria in normal unmyelinated axons is similar and their distribution appears to be random.

Wallerian Degeneration

Two hours after a crush injury, no significant abnormalities are present by phase or electron microscopy.

The onset and extent of axon and myelin disintegration vary widely in individual fibers examined 12 to 36 hours after crush injury. Thus, a few fibers show extensive axon breakdown and demyelination at 12 hours, whereas some fibers appear normal as late as 36 hours. However, in a given myelinated fiber, the earliest alterations are usually found at nodes of Ranvier 12 to 24 hours after crush, as illustrated in Fig. 4. Although terminal myelin loops and Schwann cell processes are often normal, the axon membrane may show focal alterations. Within axoplasm, there are oval vesicular bodies of varying densities of which some are continuous with mitochondria on serial section. Axon filaments may be replaced by zones of granularity, and tubules of endoplasmic reticulum may be absent or show focal dilatation. Essentially similar alterations are seen focally in unmyelinated axons 12 to 24 hours after crush, as shown in Fig. 5. The examination of many serial sections from experimental and control nerves greatly facilitated the identification of these early, ultrastructural abnormalities, some of which may resemble preparative artifacts.

These early ultrastructural abnormalities, previously reported in part by others (28, 27, 14, 11, 12), are often accompanied by the accumulation within axoplasm of numerous profiles which are morphologically similar to mitochondria (Figs. 6 to 12, 14, 15). The phase microscopic appearance of these focal collections of mitochondria (Figs. 7, 10) is characterized in serial sections by the presence of numerous thread-like and granular densities within paranodal and nodal axoplasm which often shows focal swelling (Fig. 10). These accumulations may extend through the entire

FIGURE 4

Longitudinal section, node of Ranvier, stained with lead hydroxide, 24 hours after crush. The mitochondrion in the nodal axoplasm is continuous on serial section with the irregular profile to the left and the dense body to the right which shows linear and punctate areas of increase density. Above, in the figure, a round body of uniform density and another dense body are in close relationship to the axon membrane between the terminal processes of adjacent Schwann cells (*SC*) at the node. Zones of granular density replace axon filaments and profiles of agranular endoplasmic reticulum. The terminal myelin lamellae and Schwann cell cytoplasm appear normal. × 68,000.

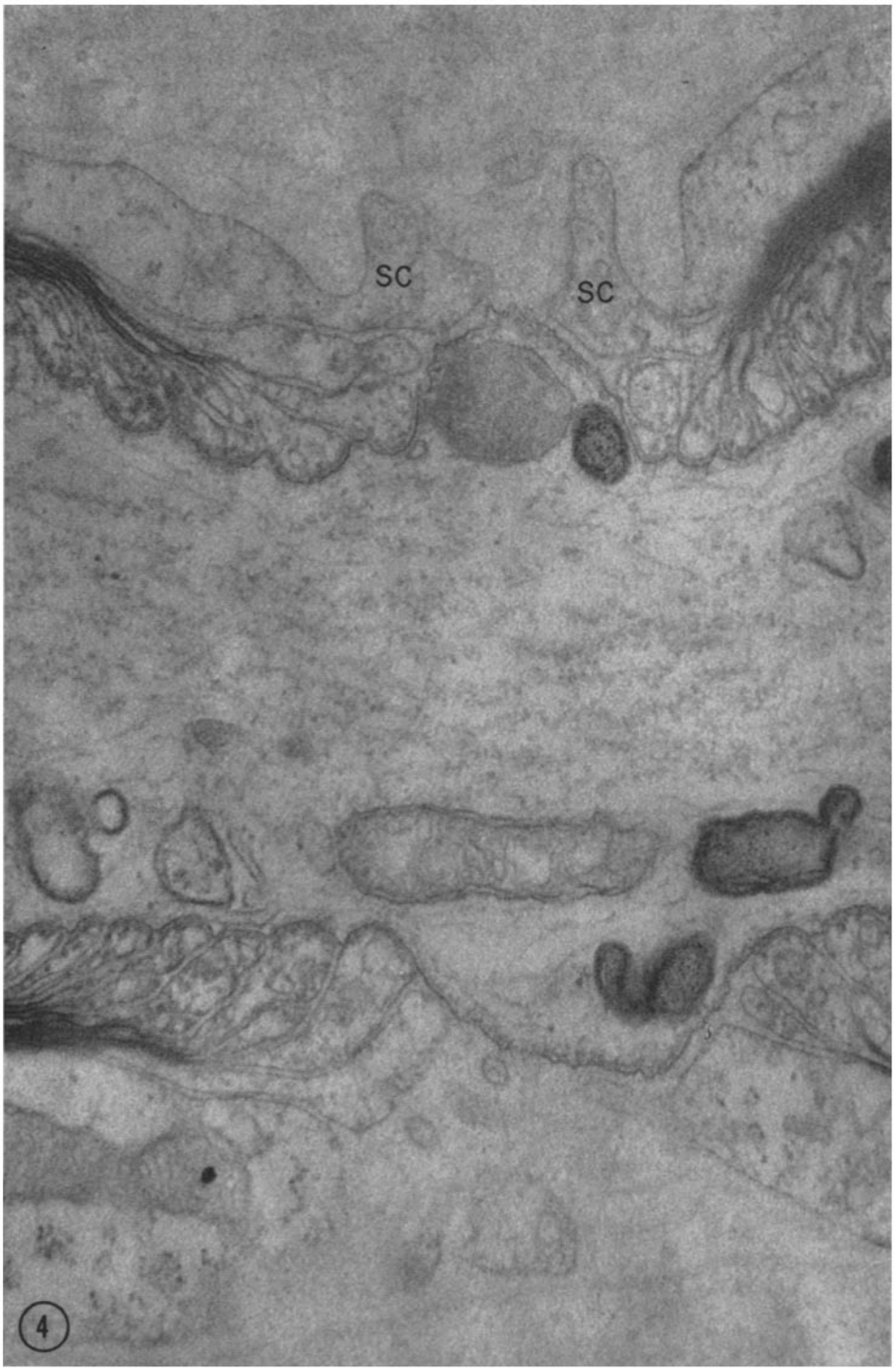
SC
SC
4

node, but are generally restricted to the distal paranodal region. Although most common in large myelinated fibers, they may be seen paranodally in smaller myelinated fibers and, rarely, in unmyelinated axons (Figs. 10 to 12, 14, 15). Counts of Ranvier nodes in serial longitudinal sections at variable intervals of time after the crush injury show that this paranodal mitochondrial aggregation is transient (occurs in 7, 28, 22, and 6 per cent of nodes at 12, 24, 36, 48 hours, respectively, and is not seen at 72 or 96 hours) and, at a given interval, is randomly distributed along the 5 to 7 mm length of nerve utilized in this study.

When examined by electron microscopy, paranodal regions showing this accumulation of mitochondria exhibit a number of distinctive features. Fragmentation, distortion, and retraction of terminal myelin loops (Figs. 6, 9) usually accompany the focal axonal swelling, although in internodal regions the myelin sheath and axon Schwann cell membrane may be normal (Fig. 12). The axoplasm itself is packed with mitochondria. They are bounded by a double membrane, the inner of which is folded longitudinally (cristae), and the matrix may contain zones of increased density. In contrast to mitochondria in normal axoplasm, they are frequently oriented tangentially or perpendicular to the fiber axis (Figs. 6, 8, 9, 11) and may be branched. Numerous variations in size, shape, and arrangement of cristae are present (Figs. 8, 9, 11, 12). In addition to the mitochondria, there are numerous oval or irregular dense bodies which frequently are arranged in rows and appear to be more numerous adjacent to the axon surface (Figs. 6, 8, 9). Lamellae are often observed but no characteristic period can be defined. Other zones in these bodies show punctate areas of increased density (Figs. 9, 11). Study of serial sections shows that some of these bodies are continuous with the mitochondria described above. The axon also contains filaments and vesicles of varying size. Finally, axoplasm with filaments, endoplasmic reticulum, and the usual distribution of normal mitochondria can be identified both proximal and distal to many of these paranodal regions.

Similar focal collections of mitochondria are occasionally found in unmyelinated axons (Figs. 14 and 15). These axons may show striking, focal enlargement (Figs. 13 and 14), and numerous discontinuities are present in the axon membrane. In many regions adjacent to the axon surface, there are vesicular profiles, a few of which may be continuous with mitochondria (Fig. 15). Dense bodies and irregular profiles containing zones of varying density are also present and are similar to those found in paranodal regions of myelinated fibers. A few of these profiles are continuous with adjacent mitochondria, many of which show the same variations in orientation, shape, and arrangement of cristae as described above.

During the later intervals utilized in this study (36 to 96 hours after crush), two observations on the axoplasm of myelinated fibers seem pertinent. First, there are numerous discontinuities in the nodal and paranodal axon membrane. They frequently occur adjacent to irregular or oval profiles, some of which appear to contain vesicles (Fig. 16). Secondly, as Vial showed (28), swelling of axonal mitochondria is commonly observed in zones of axoplasm characterized by a loss of filaments and the presence of irregular areas of granular or homogenous density (Fig. 17).

Controls

Light, phase, and electron microscopic study of serial sections of nerves from sham-operated control guinea pigs revealed no significant abnormalities in axons, axonal mitochondria, or myelin sheaths distal to the operative site.

DISCUSSION

The observation of transient, focal accumulation of profiles morphologically similar to mitochondria during a pathological process resulting in axon

FIGURE 5

Unstained, longitudinal section of a Schwann cell with unmyelinated axons, 24 hours after crush. Although the axonal mitochondria appear normal in this plane of section, several dense bodies are present. The endoplasmic reticulum is focally dilated (arrow) and axon filaments are fragmented. The larger diameter and horizontal array of cristae in Schwann cell mitochondria (*M*) are also shown. × 27,000.

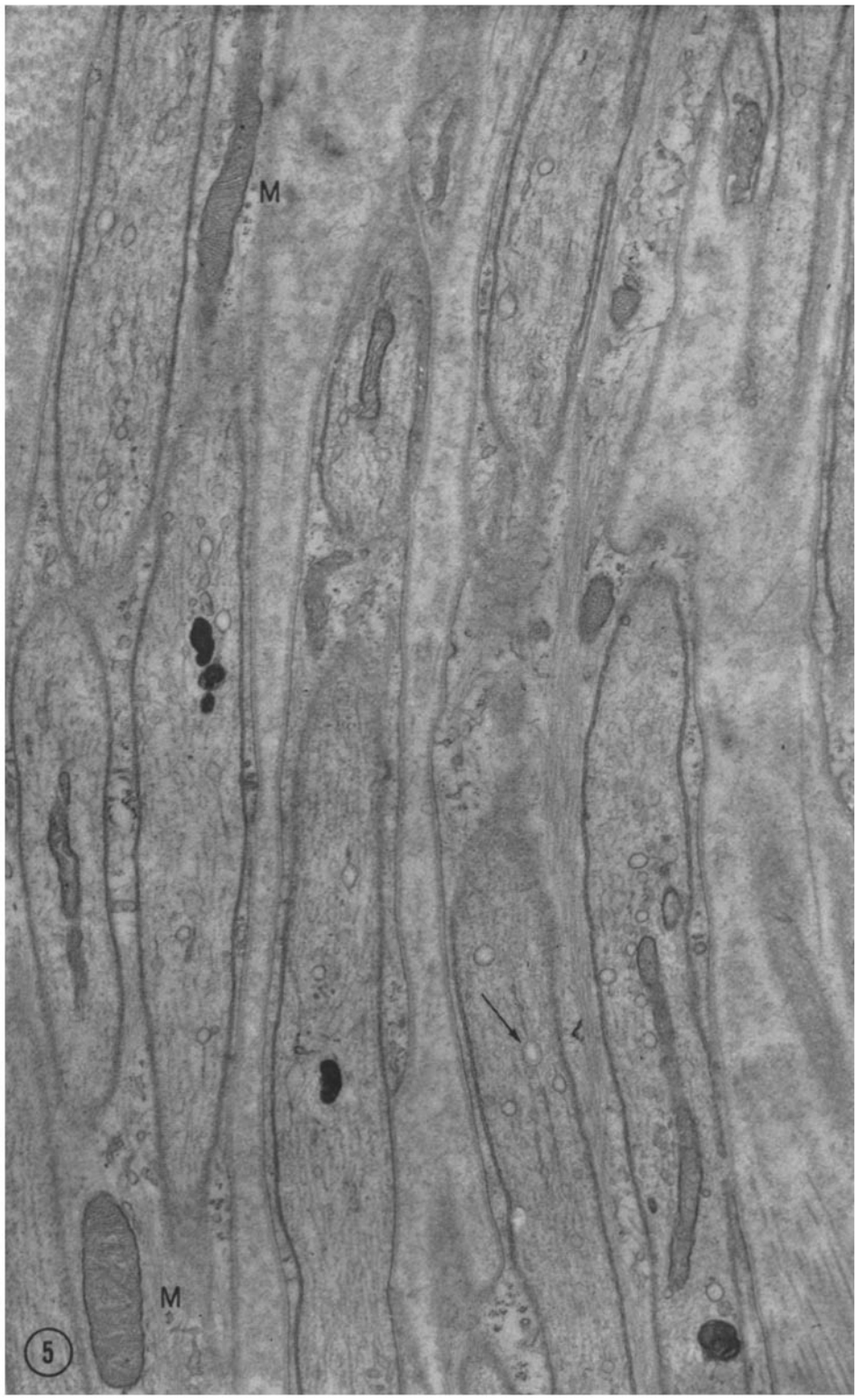
M
M
5

disintegration has not been reported previously and deserves critical appraisal.

The electron microscopic appearance of axonal mitochondria in our normal and control material is not perfectly uniform (reference 30 as well as Figs. 2, 3). Variations in mitochondrial ultrastructure may result from the slow penetration of or extraction by osmium tetroxide during the *in situ* and subsequent immersion fixation which was found necessary to prevent mechanical distortion and to produce uniform myelin preservation; they may also be due to the plane of section (22, 21). However, these slight ultrastructural variations do not interfere with the identification of axonal mitochondria or their comparison with the profiles found paranodally during Wallerian degeneration. Thus, the size, limiting double membrane, and internal structure of these profiles are characteristic of mitochondria in general (22) and also of neuronal mitochondria (23).

Although the electron microscopic appearance of mitochondria is currently used for their morphological identification, it seemed desirable to confirm the identity of these paranodal profiles by light microscopic examination of sections of nerves fixed in a different medium and stained by a method for demonstrating mitochondria. Single axonal mitochondria are difficult to identify because of their size and the resolving power of the light microscope; however, collections of red granules and threads, resembling mitochondria in other cells, are present in paranodal zones of sciatic nerves, 24 hours after crush, which were fixed in acrolein, embedded in wax, sectioned at 4 microns, and stained by the Cason method (5). Similar paranodal collections of red threads and granules are not present in sham-operated control nerves prepared by the same method.

The appearance of more mitochondria in a given plane of cross- or longitudinal section might result from folding, segmentation, or migration of pre-existing mitochondria. The first two mechanisms could explain an increase in the number of profiles seen in a single section, but not accumulations that occupy the full axonal circumference over a 30-micron length of paranodal axoplasm. Since changes in size, shape, and position of mitochondria have been observed in living cells (16), the migration of axonal mitochondria in the degenerating nerve segment distal to a crush injury might produce the transient, paranodal accumulations observed in this study. Although the distribution of mitochondria proximal and distal to these collections appears to be normal, accurate data on the individual length and internodal distribution of normal axonal mitochondria are not available due to the limited resolving power of the light microscope and the difficulty of orienting longitudinal thin sections through an entire mitochondrion. However, if an axon 6 microns in diameter with an internodal length of 600 microns contained 300 mitochondria measuring 0.2 microns by 3 microns, migration of 35 to 70 per cent of these mitochondria to the paranodal region could result in a paranodal accumulation comparable to that described in

FIGURE 6

Longitudinal section of paranodal axoplasm in the distal segment of a Ranvier node, stained with lead hydroxide, 24 hours after crush. The area shown is similar to that outlined in Fig. 7. The terminal myelin loops at the axon surface are fragmented and retracted (single arrows). The axoplasm contains irregular bodies of varying size and density as well as numerous mitochondria which may show branching (double arrow). Axon filaments are also present. A serial section of the outlined area in this figure is shown in Fig. 8. × 16,000.

FIGURE 7

Phase micrograph of a 2-micron, longitudinal section of a node Ranvier, 24 hours after crush. Numerous thread-like and granular densities are present in the distal paranodal axoplasm shown in the right portion of the figure. The axon diameter at the node is decreased; there are a few similar densities in the proximal paranodal axoplasm which is indented by myelin loops and ovoids that are normal variations in myelin sheath contour. × 2200.

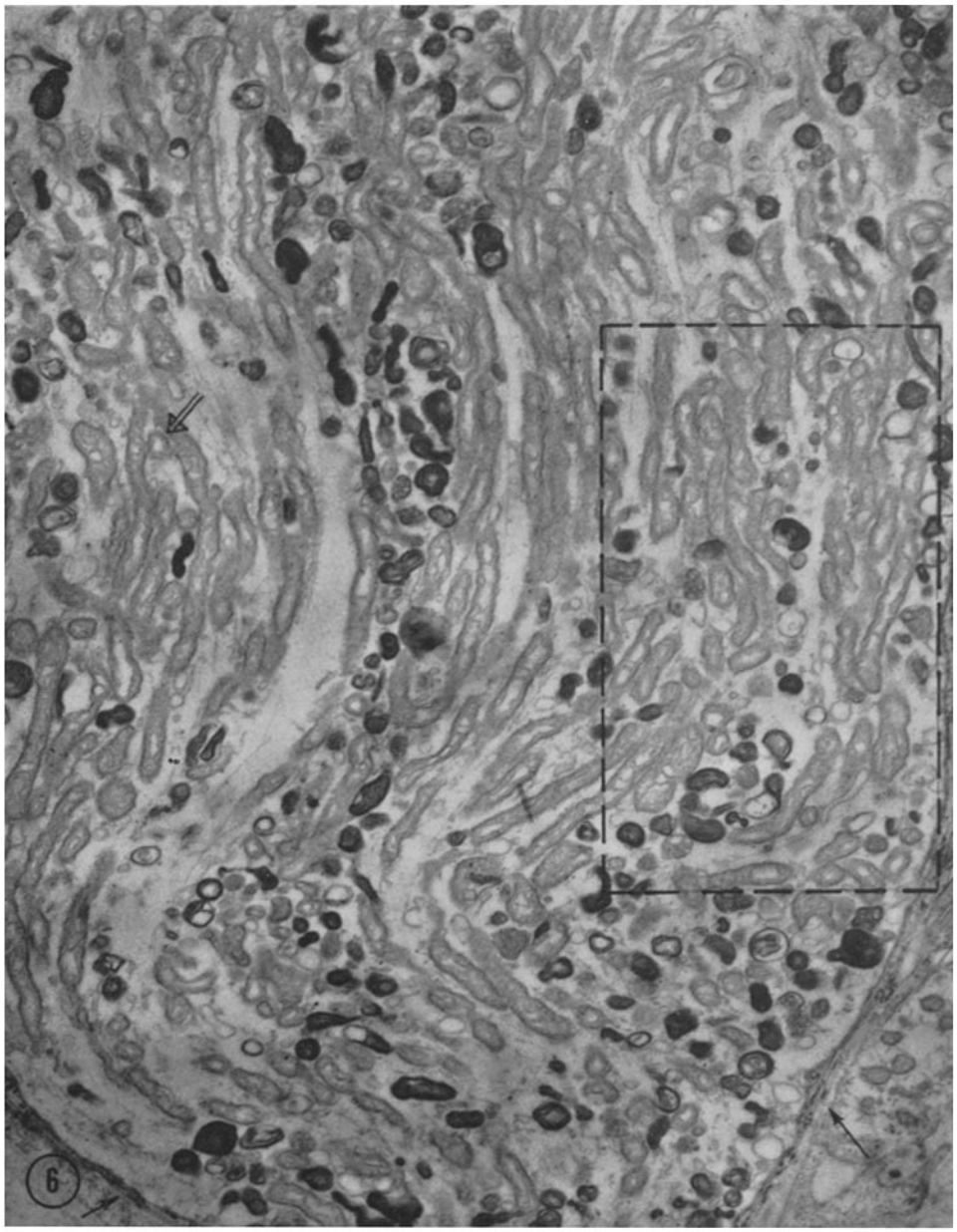
6

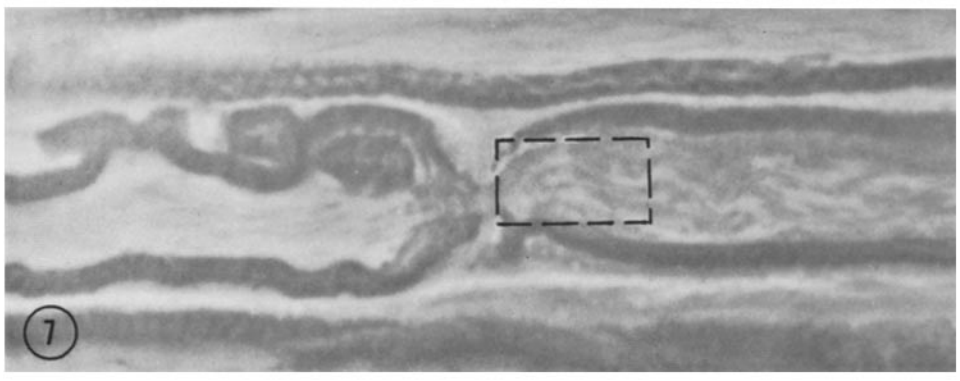
7

this study without significantly changing the observed "normal" (0 to 4 mitochondrial profiles per thin section of axon) distribution proximally or distally in a single thin section. Although the number of mitochondria per internode and the length of a mitochondrion are only approximate estimates based on electron microscopic study of normal guinea pig sciatic nerves, these figures would have to be changed very substantially in order to invalidate this migration hypothesis by electron microscopic study.

Finally, the formation of paranodal collections by the development of new mitochondria is also consistent with our observations and is of particular interest because the morphogenesis of axonal mitochondria is not yet clearly understood. Several possible sites of mitochondrial formation deserve brief consideration. First, the accumulation of mitochondria along with vesicular profiles adjacent to the axon membrane may indicate that this region is important in the formation of axonal mitochondria as Geren and Schmitt suggested in their observations on lobster axon (10). The rapid disintegration of the sparsely distributed endoplasmic reticulum in axons within 24 to 36 hours of crush injury and the lack of convincing evidence to date that mitochondria originate from the endoplasmic reticulum indicate that this organelle is not important in the formation of axonal mitochondria during Wallerian degeneration. The derivation of mitochondria from disintegrating myelin lamellae also deserves consideration. The occurrence of mitochondrial collections in unmyelinated axons and in axonal regions where both the axon membrane and adjacent myelin appear normal suggests that myelin lamellae do not play a significant role in the formation of these axonal mitochondria. Furthermore, because of their perinuclear, internodal concentration, Schwann cell organelles seem equally unlikely as an important source of paranodal axonal mitochondria. Napolitano and Fawcett, in a study of brown fat, observed an increase in the length and number of mitochondria during the formation of lipid. The ends of some mitochondria contained few cristae and it was suggested that these ends might represent zones of growth (21). Although a similar appearance has not been encountered in our observations to date, elongation preceded or accompanied by division of pre-existing mitochondria may be a possible mechanism of mitochondrial proliferation in axons, and could also explain the focal accumulations reported in this study.

The mitochondrial origin of some of the vesicular profiles and dense bodies observed paranodally is suggested by their continuity in serial section. The segmentation of mitochondria observed 12 to 36 hours after crush could result in molecular rearrangements within limiting membranes and cristae which might then be responsible for the zones of increased density seen in many axonal profiles. The remainder of these profiles may be derived from nodal multivesicular bodies (25), altered axon membrane, and myelin lamellae in paranodal zones, or altered Schwann cell constituents in unmyelinated axons with foci of axon–Schwann cell membrane discontinuity.

All paranodal collections, regardless of topographic location or the interval after crush injury, contained normal mitochondria, dense bodies, and vesicles in approximately the same proportion when examined by electron microscopy. This observation suggested that the distribution of these accumulations along the segment of nerve prepared for electron microscopic study (5 to 7 mm) and the proportion of nodes showing this change at each interval could be estimated by counting nodes (*i.e.* Fig. 7) in longitudinal section by phase microscopy. The essentially uniform appearance of these paranodal collections during the interval in which they occur probably is a manifestation of the marked variation in the degree of axonal disintegration observed in different fibers at the

FIGURE 8

A serial section of the same node shown in Fig. 6, stained with lead hydroxide. Many normal mitochondria are present although the appearance of their limiting membranes and cristae varies with the plane of section. Irregular bodies with linear and punctate areas of increased density and vesicular profiles are present in rows or nests and may be continuous with mitochondria (arrow). × 38,000.

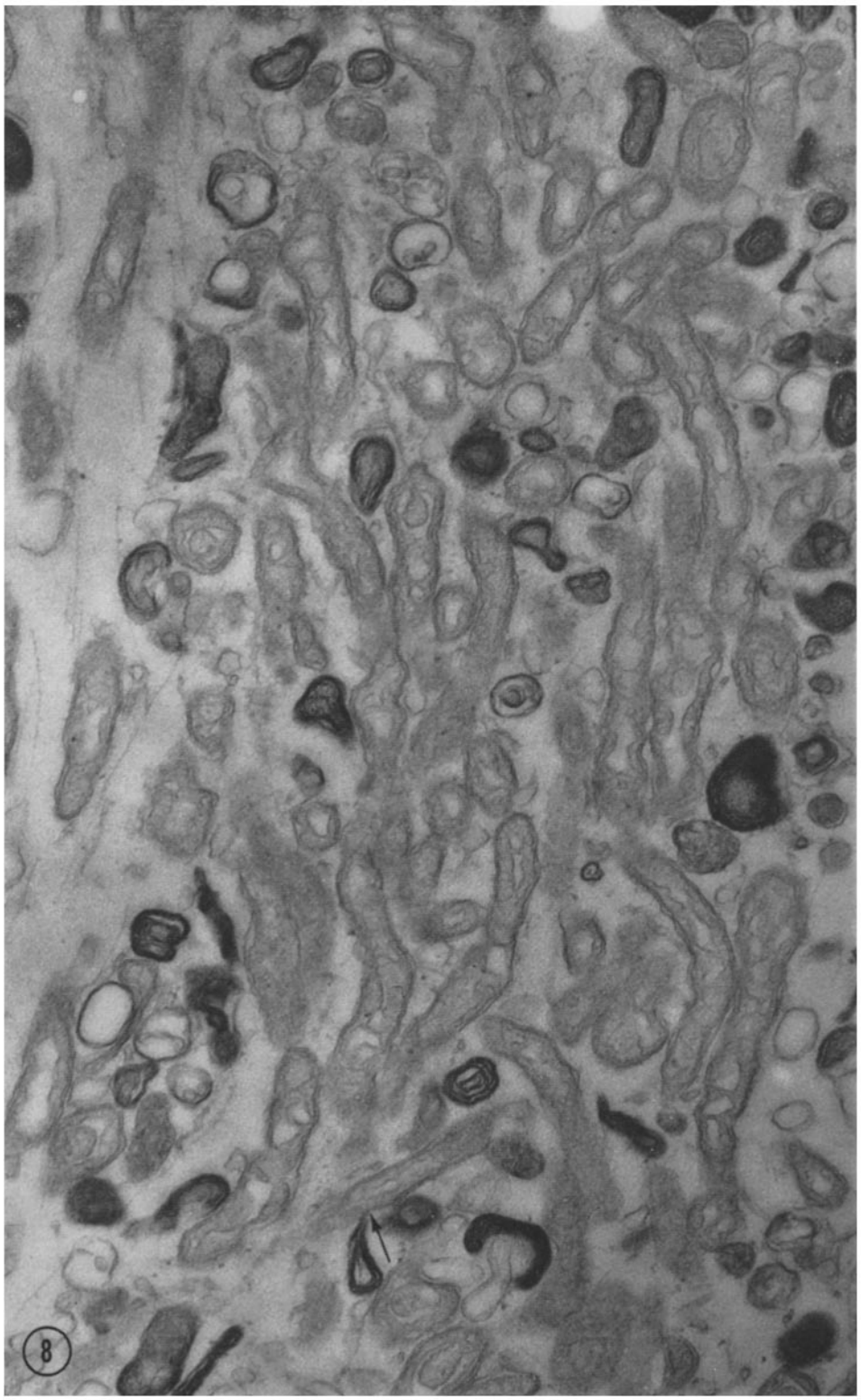
8

same interval; it could also result from sampling. Further study of serial sections of paranodal regions at more frequent intervals from 12 to 48 hours after crush should help clarify the origin of the mitochondria and their sequential alterations within these accumulations.

Alterations in axonal mitochondria have been described in Wallerian degeneration, experimental allergic encephalomyelitis, and the experimental demyelinating lesion accompanying cerebrospinal fluid exchange. Vial, in a study of the early stages of Wallerian degeneration (28), observed mitochondrial swelling and fragmentation within 48 hours of nerve section, and essentially similar results were reported by Honjin, Nakamura, and Imura (14). In a study of allergic encephalomyelitis in guinea pigs sacrificed at the onset of clinical signs, Condie and Good described an increase in the number of axonal mitochondria in myelinated central nerve fibers as the earliest recognizable abnormality which preceded subsequent disruption of cristae and mitochondrial vacuolization (7). They also suggested that degeneration of axonal mitochondria might lead to the demyelination observed in this disease. However, the initial increase in mitochondria is not documented by serial-section study and the characteristic double limiting membrane and cristae are not clearly shown in their illustrations. Also, the possible role of preparative artifacts and other origins of axonal profiles during a disease process are not considered. Axons with numerous small mitochondria were described by Luse and McDougal in peripheral nerves and spinal cords of rabbits with allergic encephalomyelitis (18). These authors indicate that similar axons showing mitochondrial multiplication are observed following the crushing or sectioning of peripheral nerves and experimental puncture wounds in the brain, and they interpret this appearance as an axon "growth cone." The conclusion that mitochondria have multiplied does not seem justified from the data presented, and our observations suggest that accumulations of axonal mitochondria can result from cellular alterations other than axonal sprouting. In their observations on the experimental demyelinating lesions produced in cats by cerebrospinal fluid exchange, Bunge, Bunge, and Ris described an increased number of mitochondria in two axons, one of which was demyelinated, 29 hours postoperatively (4). Although they are not illustrated, a review of additional observations suggests that axonal mitochondria may also accumulate during this process (3). Finally, Cauna and Ross, in a description of the fine structure of Meissner's touch corpuscles in human fingers, illustrated nerve terminals with numerous mitochondria of varying size and density, some of which showed dense concentric membranes (6). A continuous turnover of mitochondria at these endings was suggested as a possible explanation of this finding.

Correlation of our results with biochemical and physiological data obtained during Wallerian degeneration is difficult at the present time, since observations during the first 72 hours after section are frequently not included (19, 20, 24, 26) or the experimental technique utilized precludes localization of the reported abnormalities to mitochondria in axoplasm (1, 15). However, in a recent histochemical study of oxidative enzymes, Friede found no succinic dehydrogenase, DPN, or TPN diaphorase activity in the degenerating distal portion of rat sciatic nerve axons 12 hours to 50 days after transection (9). Finally, although physiological and biochemical study of single fibers during Wallerian degeneration would provide data of great interest, isolation and observation of them in artificial media may result in ultrastructural alterations in mitochondria similar to those already reported by Duncan and Hild in tissue cultures of cerebellum (8).

FIGURE 9

Longitudinal section of distal paranodal axoplasm, stained with lead hydroxide, 24 hours after crush. Numerous normal mitochondria are located in the axon along with a few, irregular, dense bodies and vesicular profiles, most of which are located near the axon surface. Adjacent to the node, several discontinuities are present in the axon membrane (single arrows). Within the Schwann cell (*SC*), the terminal myelin loops are replaced over a long distance by mitochondria, and dense bodies and are only apparent in the upper right portion of the figure (double arrow). × 50,000.

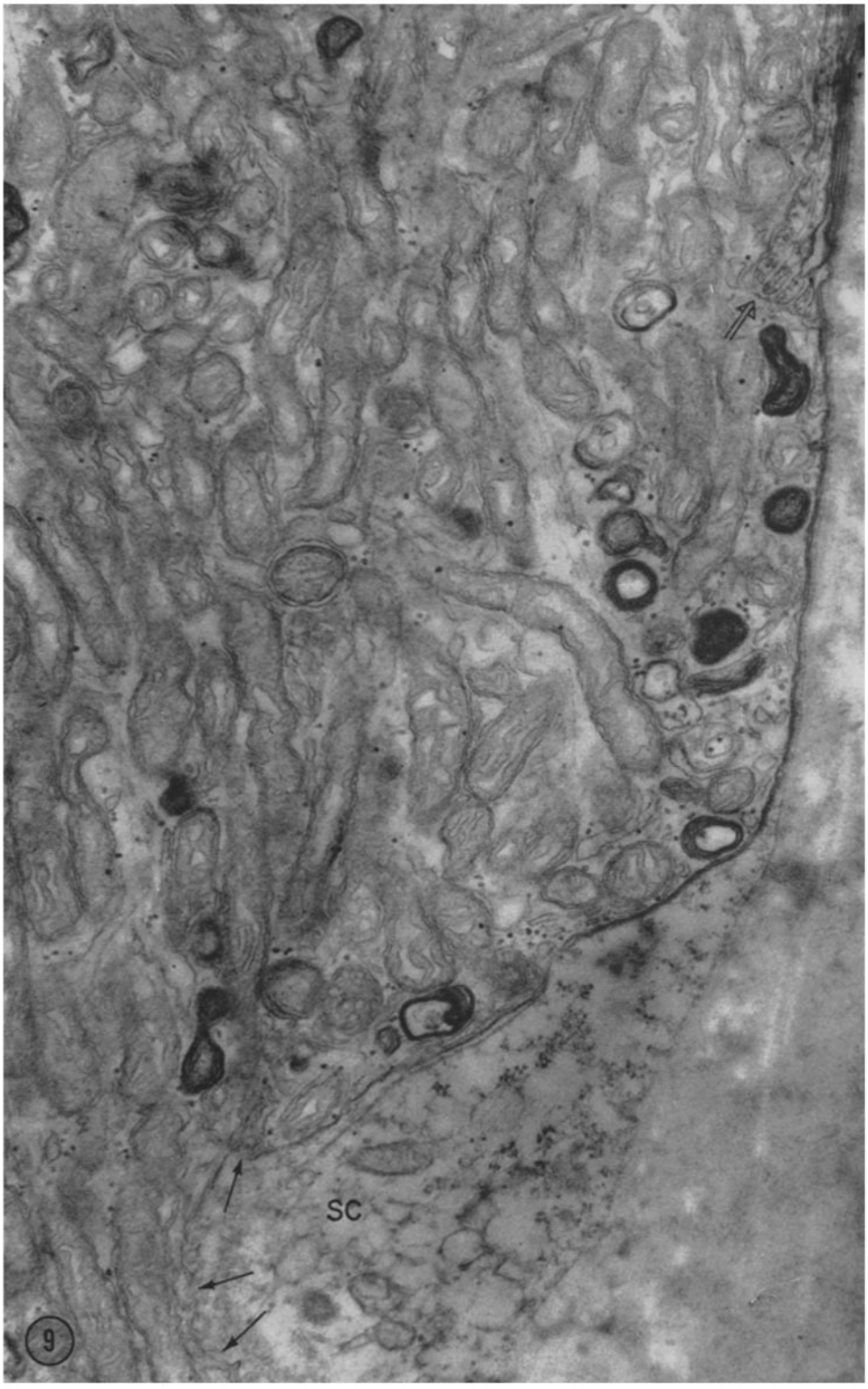
SC
9

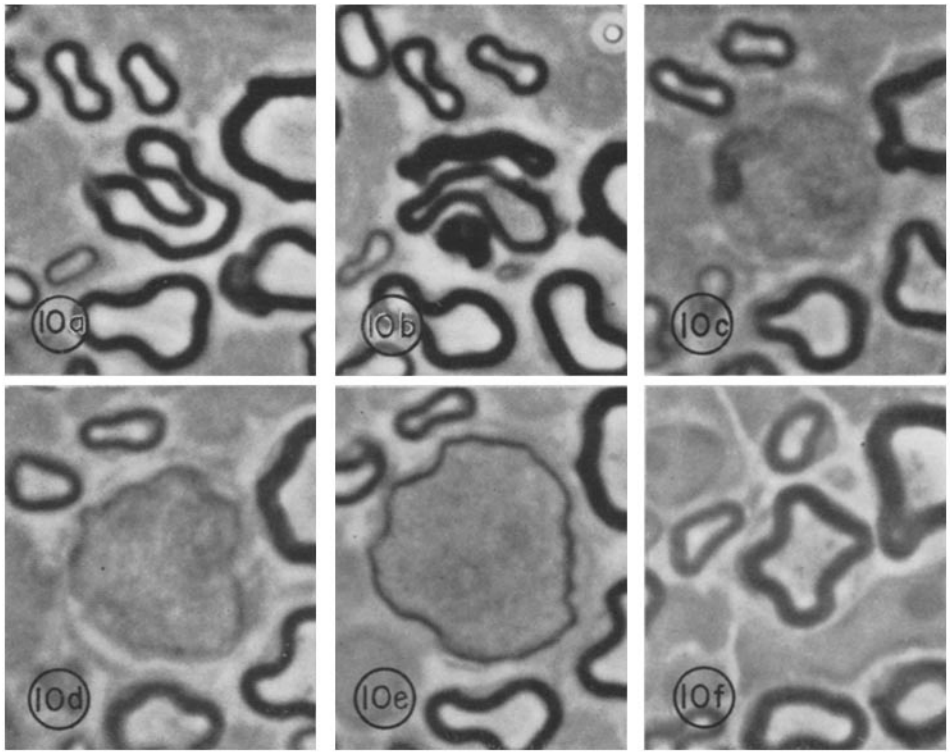

FIGURE 10

Phase photomicrographs of selected, 2-micron, serial cross-sections of the same fiber through a node of Ranvier, 24 hours after crush. The axon in (*a*), although indented by a loop of myelin, is normal proximal to the node. In the proximal paranodal region shown in (*b*), areas of increased density are present in the axon. A long myelin fold and a myelin ovoid are also present paranodally in the same Schwann cell. In (*c*), just proximal to the node, a myelin ovoid is adjacent to the axon which is filled with granular densities. Just distal to the node in (*d*) myelin partially surrounds the axon distended by similar densities which are also present in (*e*). Further distally in the paranodal region (*e*), the axon shows greater enlargement and is now completely surrounded by a thin rim of myelin. The transition distally from this appearance to normal axon and myelin sheath shown in (*f*) was studied electron microscopically and is illustrated in Fig. 11. × 3000.

This material was presented in part at the 37th Annual Meeting of the American Association of Neuropathologists, June 11, 1961.

Dr. R. Sidman kindly fixed experimental and control guinea pig sciatic nerves in acrolein, embedded them in wax, and stained them by the Cason method.

This study was supported by a research grant (C-4955) from the National Cancer Institute and a Special Fellowship (BT-404) from the National Institute of Neurological Diseases and Blindness, National Institutes of Health, Bethesda, Maryland.

The excellent technical assistance of Mr. John Michaels and the photographic suggestions of Mr. Frank Mason are gratefully acknowledged.

Received for publication, August 14, 1961.

REFERENCES

1. ADAMS, C. W. M., and TUQUAN, N. A., Histochemistry of myelin II. Proteins, lipid-protein dissociation and proteinase activity in Wallerian degeneration, *J. Neurochem.*, 1961, **6**, 334.
2. ANDERSSON-CEDERGREN, E., Ultrastructure of

motor end plate and sarcoplasmic components of mouse skeletal muscle as revealed by three-dimensional reconstructions from serial sections, *J. Ultrastruct. Research*, 1959, Suppl. 1.
3. BUNGE, M. B., Personal communication. (1961)
4. BUNGE, R. P., BUNGE, M. B., and RIS, H., Electron microscopic study of demyelination in an experimentally induced lesion in adult cat spinal cord, *J. Biophysic. and Biochem. Cytol.*, 1960, **7**, 685.
10. GEREN, B. B., and SCHMITT, F. O., The structure of the Schwann cell and its relation to the axon in certain invertebrate nerve fibers, *Proc. Nat. Acad. Sc.*, 1954, **40**, 863.
11. GLIMSTEDT, G., and WOHLFART, G., Electron microscopic observations on Wallerian degeneration in peripheral nerves, *Acta Morphol. Neerl.-Scand.*, 1960, **3**, 135.
12. GLIMSTEDT, G., and WOHLFART, G., Electron microscopic studies on peripheral nerve

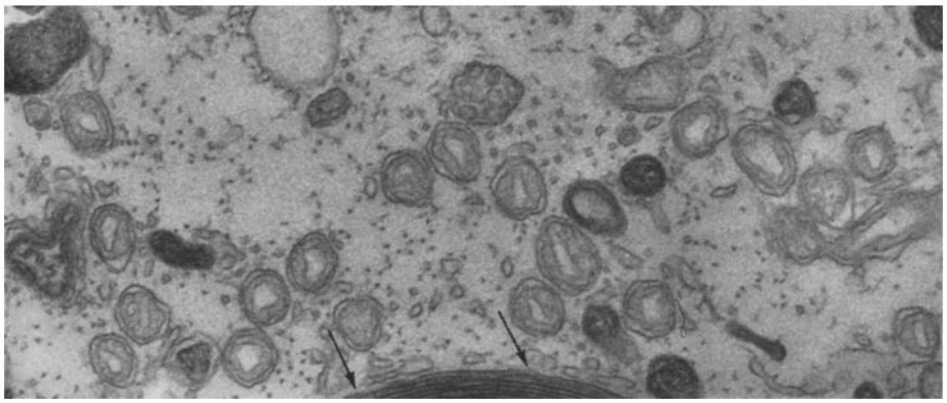

FIGURE 11

Lead hydroxide-stained cross-section of the same fiber shown in Fig. 10, distal to (*e*) and within a few microns of (*f*). At this level, numerous normal mitochondria are present in the small portion of axoplasm illustrated. A few dense bodies are also shown. Discontinuities in myelin lamellae are adjacent to vesicular profiles in axoplasm (arrows). The transition of this appearance to normal axoplasm and lamellar myelin further distally was observed in serial sections. × 56,000.

5. CASON, J. E., A rapid one - step Mallory-Heidenhain stain for connective tissue, *Stain Technol.*, 1950, **25**, 225.
6. CAUNA, N., and ROSS, L. L., The fine structure of Meissner's touch corpuscles of human fingers, *J. Biophysic. and Biochem. Cytol.*, 1960, **8**, 467.
7. CONDIE, R. M., and GOOD, R. A., Experimental allergic encephalomyelitis: Its production, prevention, and pathology as studied by light and electron microscopy, *in* The Biology of Myelin, (S. A. Korey, editor), New York, Paul B. Hoeber, p. 321, 1959.
8. DUNCAN, D., and HILD, W., Mitochondrial alterations in cultures of the central nervous system as observed with the electron microscope, *Z. Zellforsch.*, 1960, **51**, 123.
9. FRIEDE, R. L., Transport of oxidative enzymes in nerve fibers; a histochemical investigation of the regenerative cycle in neurons, *Exp. Neurol.*, 1959, **1**, 441.
regeneration, Lunds Universitets Arsskrift, N.F. Aud. 2, Bd. 56, Nr. 16, 1960.
13. HESS, A., and LANSING, A. I., The fine structure of peripheral nerve fibers, *Anat. Rec.*, 1953, **117**, 175.
14. HONJIN, R., NAKAMURA, T., and IMURA, M., Electron microscopy of peripheral nerve fibers. III. On the axoplasmic changes during Wallerian degeneration, *Okajimas Folia Anat. Japan*, 1959, **33**, 131.
15. LEHMANN, H. L., Struktur und Funktion Peripherer Warmblüter - Nerven - Fasern Im Frühstadium der Wallerschen Degeneration, *Z. Zellforsch.*, 1960, **51**, 283.
16. LEWIS, M. R., and LEWIS, W. H., Mitochondria (and other cytoplasmic structures) in tissue cultures, *Am. J. Anat.*, 1914–15, **17**, 339.
17. LUFT, J. H., Improvements in epoxy embedding methods, *J. Biophysic. and Biochem. Cytol.*, 1961, **9**, 409.

FIGURE 12

Cross-section, myelinated fiber, stained with lead hydroxide, 24 hours after crush. Numerous normal mitochondria are present within axoplasm, along with vesicular profiles and dense bodies. Folding or branching may account for the apparent continuity of two of these mitochondria (single arrow), one of which may be continuous with a dense body (double arrow). The axon membrane, myelin sheath, and Schwann cell cytoplasm appear normal. × 49,000.

18. LUSE, S. A., and MCDOUGAL, D. B., Electron microscopic observations on allergic encephalomyelitis in the rabbit, *J. Exp. Med.*, 1960, **112**, 735.

19. MCCAMEN, R. E., and ROBINS, E., Quantitative biochemical studies of Wallerian degeneration in the peripheral and central nervous systems. I. Chemical constituents, *J. Neurochem.*, 1959, **5**, 18.

20. MCCAMEN, R. E., and ROBINS, E., Quantitative biochemical studies of Wallerian degeneration in the peripheral and central nervous systems. II. Twelve Enzymes, *J. Neurochem.*, 1959, **5**, 32.

21. NAPOLITANO, L., and FAWCETT, D., The fine structure of brown adipose tissue in the newborn mouse and rat, *J. Biophysic. and Biochem. Cytol.*, 1958, **4**, 685.

22. PALADE, G. E., An electron microscopic study of mitochondrial structure, *J. Histochem. and Cytochem.*, 1953, **1**, 188.
23. PALAY, S. L., and PALADE, G. E., The fine structure of neurons, *J. Biophysic. and Biochem. Cytol.*, 1955, **1**, 69.
24. PORCELLATI, G., and CURTI, B., Proteinase activity of peripheral nerves during Wallerian degeneration, *J. Neurochem.*, 1960, **5**, 277.
25. ROBERTSON, J. D., Preliminary observations on the ultrastructure of nodes of Ranvier, *Z. Zellforsch.*, 1959, **50**, 553.
26. TAKAHASHI, Y., NOMURA, M. and FURUSAWA, S., *In vitro* incorporation of (^{14}C) amino acids into proteins of peripheral nerve during Wallerian degeneration, *J. Neurochem.*, 1961, **7**, 97.
27. TERRY, R. D., and HARKIN, J. C., "Wallerian Degeneration and Regeneration" in the Biology of Myelin, (S. A. Korey, editor), New York, Paul B. Hoeber, 1959, 303.
28. VIAL, J. D., The early changes in axoplasm during Wallerian degeneration, *J. Biophysic. and Biochem. Cytol.*, 1958, **4**, 551.
29. WEBSTER, H. DEF., and SPIRO, D., Phase and electron microscopic studies of experimental demyelination. I. Variations in myelin sheath contour in normal guinea pig sciatic nerve, *J. Neuropath. and Exp. Neurol.*, 1960, **19**, 42.
30. WEBSTER, H. DEF., SPIRO, D., WAKSMAN, B. H., and ADAMS, R. D., Phase and electron microscopic studies of experimental demyelination. II. Schwann cell changes in guinea pig sciatic nerves during experimental diphtheritic neuritis, *J. Neuropath. and Exp. Neurol.*, 1961, **20**, 5.

FIGURE 13

Cross-section of Schwann cell containing unmyelinated axons, stained with lead hydroxide, 24 hours after crush. The axon in the center of the figure contains many small bodies of varying density. There is a zone of discontinuity in the Schwann cell membrane forming the mesaxon (single arrow) and the axon membrane may also be discontinuous (double arrow). Other axons (*A*) and the Schwann cell cytoplasm appear normal. × 22,000.

FIGURE 14

Lead hydroxide–stained serial section of the same axon shown in Fig. 13 illustrated at the same magnification. Striking focal enlargement of the axon is present at this level. Numerous normal mitochondria, dense bodies, vesicles, and filaments are present within this axon. The axon membrane and adjacent Schwann cell membrane are poorly defined in several regions and may be discontinuous (arrows). Numerous vesicles are apparent in these regions. Other axons (*A*) within the same portion of this Schwann cell appear normal. × 22,000.

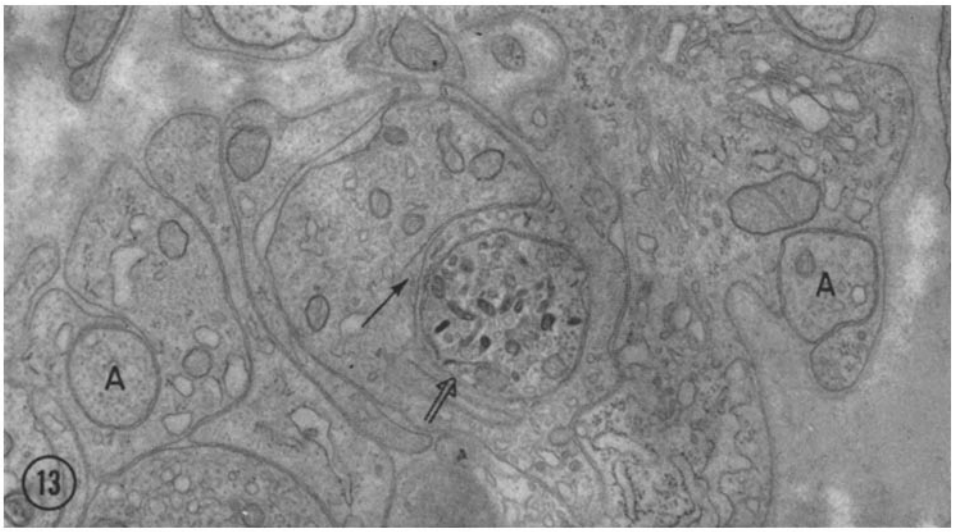
A
A
13

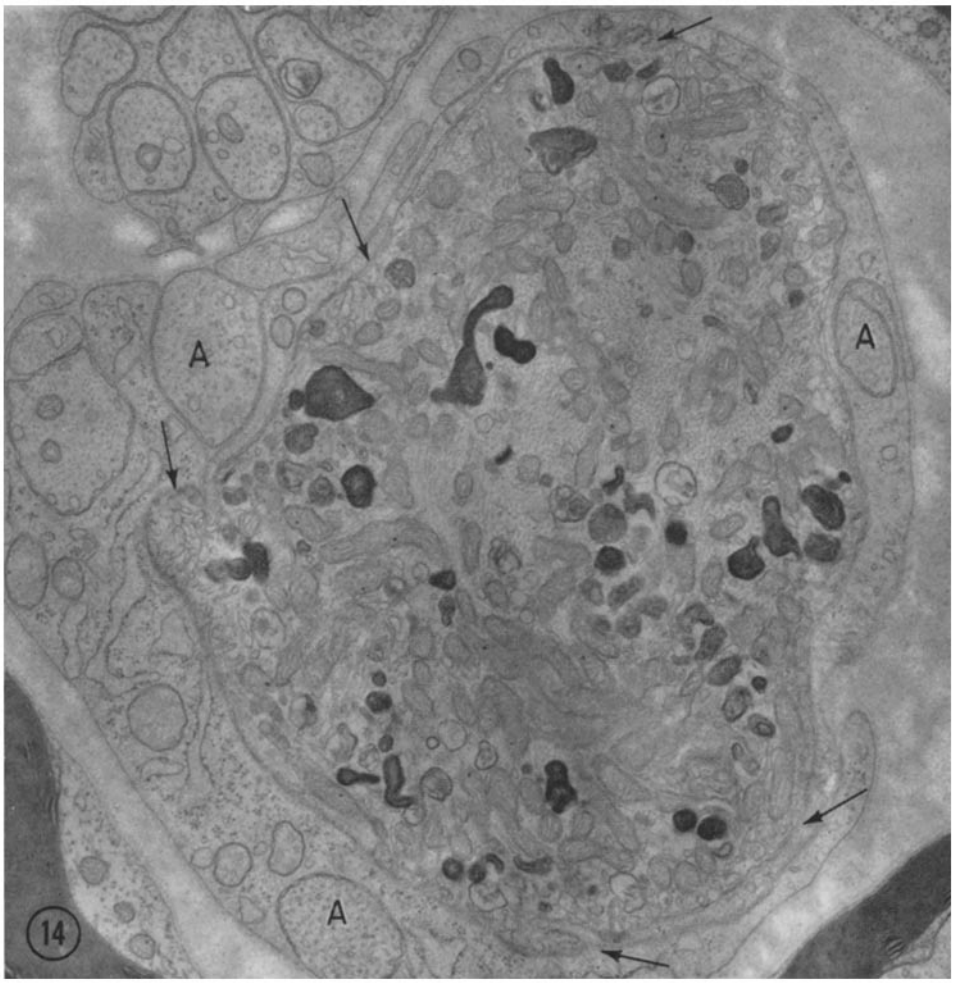
A
A
A
14

FIGURE 15

The same axon shown in Fig. 14 at higher magnification. The normal ultrastructure of many axonal mitochondria is apparent. The irregular profiles of varying density appear similar to those illustrated in myelinated axons. × 37,000.

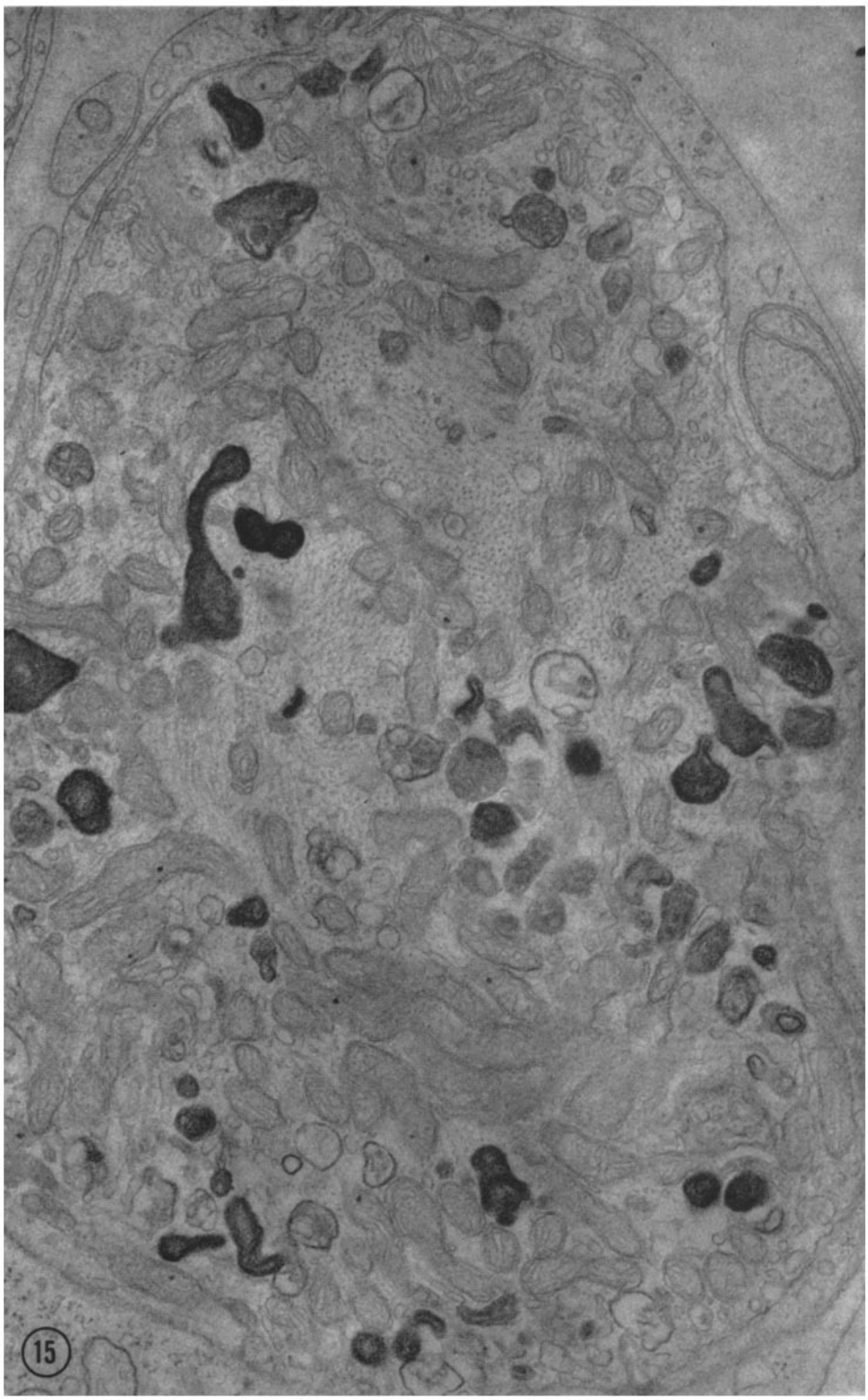
15

FIGURE 16

Lead hydroxide–stained cross-section through the terminal Schwann cell processes in the paranodal region of a myelinated axon, 36 hours after crush. Numerous focal areas of indentation and discontinuity are present in the axon membrane. Four irregular bodies within the axon are membrane-limited and contain linear or circular zones of increased density. × 37,000.

FIGURE 17

Unstained cross-section of axoplasm, 72 hours after crush. Marked swelling is present in some mitochondria. The limiting membranes are poorly defined in several areas and many cristae are replaced by circular profiles or zones of increased density (double arrow). Axon filaments and profiles of endoplasmic reticulum are replaced by areas of granular density. The axon membrane is discontinuous (single arrows) and irregular profiles are present in the Schwann cell cytoplasm (*SC*) adjacent to a myelin fragment which is not illustrated. × 37,000.


16

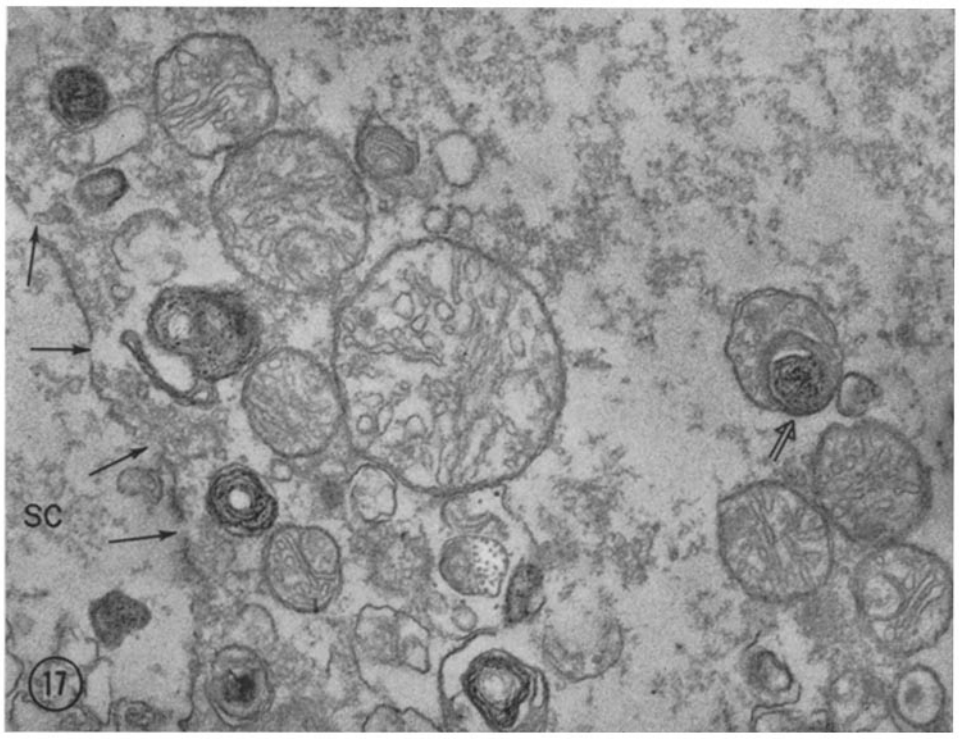
SC
17